Thin films of calcium phosphate and titanium dioxide by a sol-gel route: a new method for coating medical implants

L. -D. PIVETEAU*, M. I. GIRONA, L. SCHLAPBACH
Institut de Physique, Université de Fribourg, CH-1700 Fribourg, Switzerland
E-mail: Laurent.Piveteau@unifr.ch

P. BARBOUX, J. -P. BOILOT
Laboratoire de Physique de la Matière Condensée, Ecole Polytechnique, F-91128 Palaiseau-Cedex, France

B. GASSER
Dr h.c. Robert Mathys Foundation, CH-2544 Bettlach, Switzerland

Titanium is a commonly used biomaterial for dental and orthopaedic applications. To increase its ability to bond with bone, some attempts were made to coat its surface with calcium phosphate (CaP). This paper describes a new type of coating. Instead of a pure CaP layer, a mixing of titanium dioxide (TiO_2) and CaP is fabricated and deposited as a coating. These layers are deposited by a sol-gel route on pure titanium substrates using various pre-treatments. The method consists of mixing a solution of tetrabutyl ortho-titanate or a sol of titanium dioxide with a solution of calcium nitrate and phosphorous esters. This composite is deposited on to commercially pure titanium plates, mechanically polished or blasted with pure crystalline aluminum oxide, using the spin-coating technique. These coatings are then fired at 650 or 850 °C for various times. The samples are characterized by X-ray diffraction for their crystallinity, X-ray photoelectron spectroscopy for their surface chemical composition and scanning electron microscopy for their topography. Samples treated at 850 °C present a well-pronounced crystallinity, and a high chemical purity at the surface. The topography is strongly related to the viscosity of the precursor and the substrate pre-treatment. Possibilities to structure the outermost layer are presented.

1. Introduction

After being introduced in the 1960s by Brånemark *et al.* [1], titanium implants have gradually replaced other metallic biomaterials, like stainless steel and cobalt chromium alloys, in applications with high mechanical strength requirements, especially for dental implants. This success is due to both their chemical and biological stability, and to their mechanical properties. A very important contribution comes from the dioxide layer (TiO_2) spontaneously forming at the surface. Being very stable, it slows down the corrosion, maintaining mechanical properties and lowering material dissolution out to the tissues. Even when attacked, it only releases non-toxic and non-reactive products. The ability of titanium to replace mechanical functions of the body is broadly due to its strength. Its low weight increases the life quality of the patient and its ductility facilitates the adaptation work of the surgeon. All these properties, combined with an ability for direct adhesion to the bone without connective tissue and the lack of allergic or immunogenic reactions [2], explain the large success of titanium as a biomaterial.

Concurrently, attempts were made to fabricate materials favoring bone growth, osteoconductive materials, to reduce the convalescence period during which an implant cannot be loaded. Calcium phosphates (CaP) form a class of materials which clearly show an osteoconductive ability. Hydroxyapatite [OHAp, $Ca_10(PO_4)_6(OH)_2$], which is stable after implantation, and β-tricalcium phosphate [β-TCP, $Ca_9(PO_4)_6$], which is slowly dissolved and replaced by the growing bone matrix, are the most promising of the calcium phosphates. The bad mechanical properties of calcium phosphates limited the use of bulk material to non-load-bearing implants. For this reason, many different methods were tested to coat metallic implants, in particular titanium, with calcium phosphate layers. The main goal was to combine the mechanical properties of the metals with the osteoconductive properties of CaP. The success achieved by these methods is variable.

*Author to whom all correspondence should be addressed. From October 1, 1998, the address of the corresponding author will be: Massachusetts Institute of Technology, Department of Chemical Engineering, Cambridge, MA 02139.

Currently, the most commonly used technique for coating is plasma spraying. It has been widely studied [3, 4] and has been shown to produce premature wear loosening of the implant because of dissolution of the coating [5]. Other techniques were developed more recently, such as electrophoresis [6], pulsed laser deposition [7], electrocrystallization [8], surface-induced mineralization [9] and the sol gel technique [10, 14]. A major problem of these coatings is the mechanical weakness of the metal oxide/calcium phosphate interface. To increase the adhesion of the coating, instead of a simple juxtaposition, we propose to deposit a film formed of a mixture of TiO_2 and CaP crystallites [15, 16].

In this paper we report a new method, based on a sol gel route, to fabricate these coatings. The coated samples are characterized for their crystallinity by X-ray diffraction (XRD), for their surface chemical composition by X-ray photoelectron spectroscopy (XPS), and for their morphology by scanning electron microscopy (SEM).

2. Materials and methods

Calcium phosphate embedded in a titanium dioxide film was deposited using a sol gel route. A flow chart of the method is presented in Fig. 1.

Two types of titanium precursor were used: a 1 M solution of tetrabutyl ortho-titanate $[Ti(OBu)_4, Ti(O(CH_2)_3CH_3)_4]$ in absolute ethanol, and a sol of TiO_2. The TiO_2 sol was obtained by hydrolyzing a 1 M solution of $Ti(OBu)_4$ in absolute ethanol. Distilled water (H_2O) dissolved in absolute ethanol was carefully added to the titanium solution under strong stirring. The water was acidified with nitric acid (HNO_3) to prevent precipitation of titanium dioxide. The ratio $[H_2O]$: [Ti] was fixed at 2:1 and the ratio $[H^+]$: [Ti] at 1 : 100.

Phosphoric acid is very reactive and precipitates in the presence of calcium, even at a low concentration. To increase the concentration of our precursors, less reactive phosphorus precursors, such as phosphoric acid esters, were used. A 1 M solution of phosphoric acid esters [P(OR)] was prepared by dissolving phosphorous pentoxide (P_4O_{10}) in absolute ethanol. The very exothermic reaction is described by [17]

$$P_4O_{10} + 6(CH_3)(CH_2)(OH) \rightarrow 2(P(O(CH_2)(CH_3))(OH)_2O) + 2(P(O(CH_2)(CH_3))_2(OH)O) \quad (1)$$

A 0.5 M solution of calcium was obtained by dissolving calcium nitrate tetrahydrate $[CaNO_3 + 4H_2O]$ in absolute ethanol.

Both calcium and phosphorus were mixed together in the correct proportion to obtain a Ca/P ratio between 1.67 and 1.5. This solution was finally added either to the solution of $Ti(OBu)_4$ or to the sol of TiO_2. These final composites can be concentrated by evaporation of the ethanol.

Layers of these composites were deposited by spin coating on to commercially pure mechanically polished, or blasted with pure crystalline aluminum oxide, titanium plates. The process could be repeated several times. Between the deposition of each layer. the sample was calcined at 350 °C in air for 5 min to evaporate the remaining solvent and to calcine the remaining esters. After deposition of three or four layers, the coating was crystallized at 650 or 850 °C in air for times between 5 and 15 min (Fig. 2).

XRD was performed at room temperature using a Siemens D-500 MP diffractometer with Cu*K*, radiation (0.154 nm). Scans were performed at 40 kV and 30 mA and $2\Theta = 10$–70 with a continuous speed of $0.001\ s^{-1}$. Phase analysis was performed by comparing sample diffraction peaks to literature data [18] as well as spectra obtained from commercially pure calcium phosphates (Mathys AG. Switzerland).

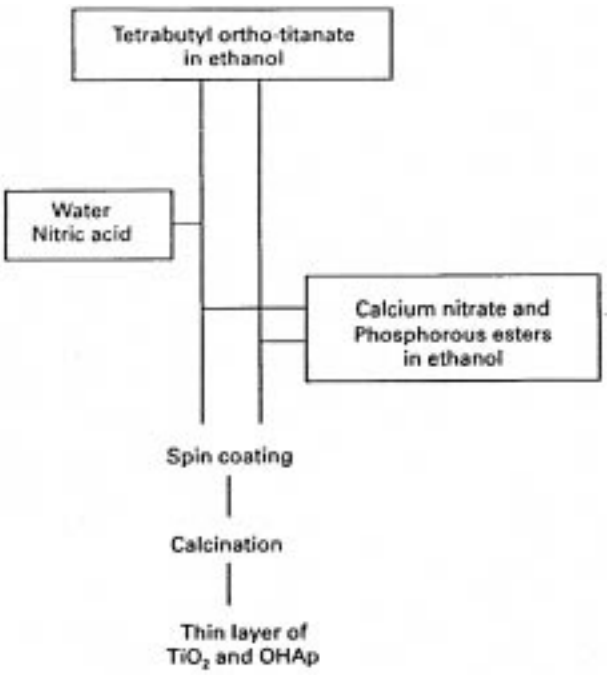

Figure 1 Schematic processing diagram for the preparation of thin layers of calcium phosphate (CaP) and titanium dioxide (TiO_2) by a sol gel route.

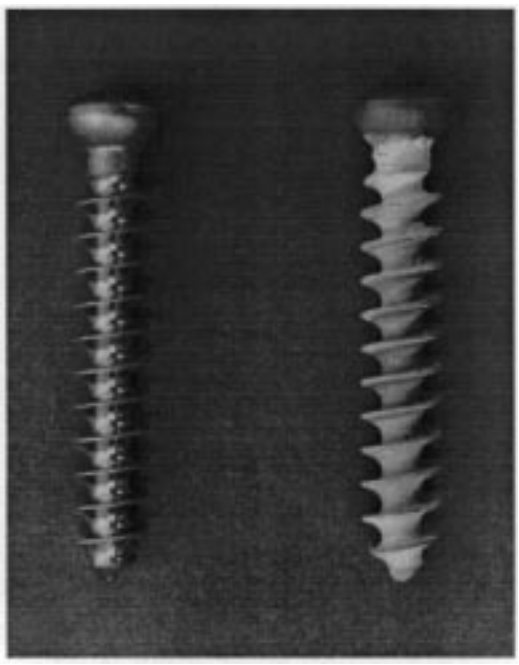

Figure 2 One CaP TiO_2 coated screw-shaped implant (right side) compared to one commercially pure titanium screw (left side).

A VG Escalab 5 X-ray photoelectron spectrometer with Mg*K*, (1254 eV) source was used to collect XPS data. The samples were analyzed using a take-off angle of 90 °C. Survey scans evaluating binding energies from 0 1000 eV, were used to determine the qualitative composition, while high-resolution measurements were performed over relevant elemental peaks to access surface chemistry. High-resolution scan analysis involved charge compensation, taking the C 1 s peak as reference (BE = 284.6 eV [19]), satellite subtraction, background subtraction, using an integral background based on the Shirley method, peak fitting, integration and division by the cross-section of the different elements, to evaluate the relative chemical composition [20].

In connection with the XPS analyses, 1 keV Ar^+ ions were used for sputter cleaning of the surfaces and for concentration depth profiling. The sputtering rate was about 0.2 nm min^{-1}.

Surface morphology was investigated using a Jeol JSM-840A and a Zeiss DMS Gemini 982 scanning electron microscope.

3. Results and discussion

3.1. XRD

Two types of coatings precursors were compared. The first one was a mixture of a titanium dioxide sol with a calcium nitrate and phosphorous esters solution (denoted sol); the second one was a mixture of solutions of tetrabutyl ortho-titanate, calcium nitrate and phosphorous esters (denoted solution). Their relative concentrations are given in Table I.

In order to increase the coating thickness and, therefore, that part of the XRD signal emanating from the coating, precursors were concentrated to enhance their viscosity.

A qualitative phase analysis was performed for various temperatures and various durations of crystallization. Fig. 3 shows the phase evolution with temperature of the coatings prepared with the sol. The structural evolution begins from an amorphous or poorly crystallized film in the unfired state (350 °C), with a crystalline TiO_2 anatase phase appearing at 650 °C and a more complicated structure containing TiO_2 anatase, TiO_2 rutile, apatite and β-TCP at 850 °C. The difference in relative intensities of the substrate peaks between Fig. 3 and Figs 4–6 originates from the sample pretreatment. Both structures are α-phase titanium but with different preferential orientations. Changing the duration of firing between 1 and 15 min for a temperature of 850 °C does not produce any change in phase composition (Fig. 4). The only evolution is the relative increase of the rutile TiO_2 signal. It seems that the presence of the rutile phase is strongly related to the thermal oxidation of the substrate. This is confirmed by the complete absence of this rutile TiO_2 phase on the diffraction patterns obtained from powders of pure mixing, independently of the calcination time.

TABLE I Relative concentrations of titanium, calcium and phosphorus in a sol and in a solution

	Ti	Ca	P
Sol	1	0.76	0.46
Solution	1	0.38	0.23

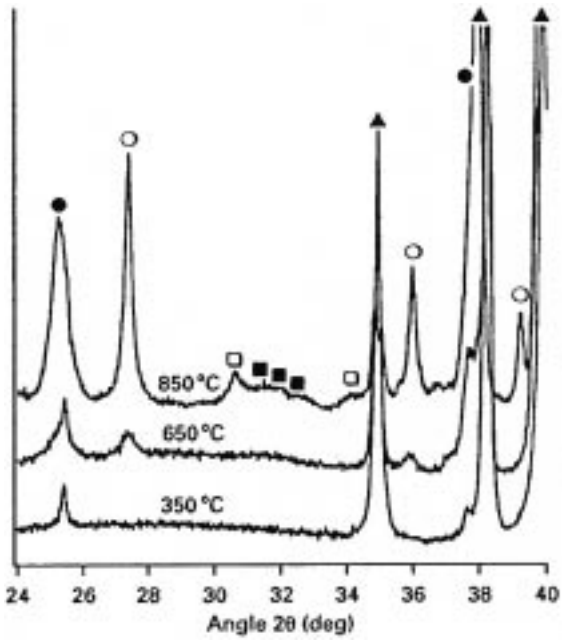

Figure 3 X-ray diffraction pattern of a coating prepared with a sol and crystallized at 850 °C for 10 min at various temperatures. (●) TiO_2 anatase, (○) TiO_2 rutile, (■) OHAp, (□) β-TCP, (▲) substrate.

The structural evolution of the film prepared with the solution (Fig. 5) is quite different. It also starts with an amorphous or poorly crystallized structure. At 650 °C, calcium titanate ($CaTiO_3$), with the perovskite structure, is formed. Further heat treatment progressively destroys this phase and replaces it with the same phase composition as for a film prepared with a sol. For a constant temperature of 850 °C and short firing time, a different phase composition from that of the film prepared with a sol precursor is observed (Fig. 6). An

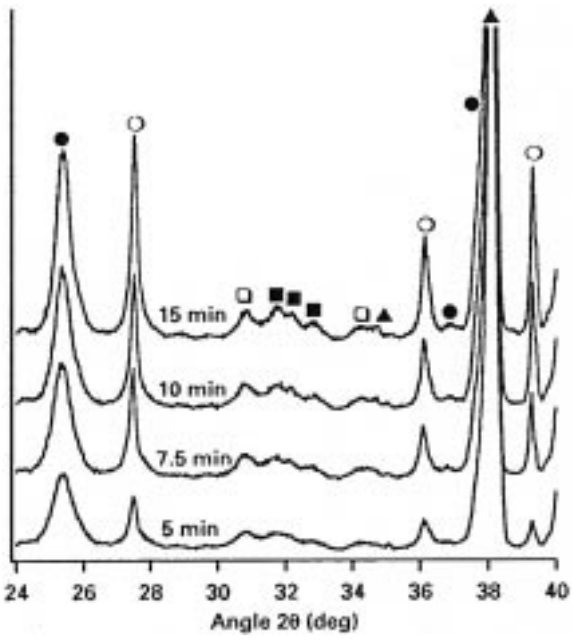

Figure 4 X-ray diffraction pattern of a coating prepared with a sol and crystallized for 850 °C for various times: (●) TiO_2 anatase, (○) TiO_2 rutile, (■) OHAp (□) β-TCP, (▲) substrate.

additional $CaTiO_3$ phase is formed which slowly disappears.

This difference in behavior can be explained by the much higher stability of titanium dioxide compared to that of tetrabutyl ortho-titanate. The calcium is present in the precursor as ions. In the case of the solution. $CaTiO_3$ is immediately formed by the reaction of tetrabutyl ortho-titanate molecules with calcium ions. The esters of the phosphoric acid must first be calcined before reacting with calcium and forming calcium phosphate. In the case of the sol, calcium cannot react easily with the very stable TiO_2 colloidal particles.

3.2. XPS

A typical XPS survey spectrum is shown in Fig. 7. No distinguishable impurities are present at the surface. The relatively strong C 1 s signal can be attributed to surface contamination by adsorbed hydrocarbon molecules, which is a normal observation for air-exposed surfaces. This is confirmed by the decrease of the C 1 s signal (of the order of the noise level) after sputtering to a depth of $\sim$ 2 nm (see Fig. 10 below). No other contaminants were observed at the surface.

A representative high-resolution spectrum of O 1 s with a pass energy of 20 eV, which corresponds to a Au 4 f FWHM of 1.2 eV, is shown in Fig. 8. It exhibits two main components at 529.6 and 531.1 eV. The first one is attributed to TiO_2, and the second one to PO_4 [21]. A quantitative analysis obtained by comparing the surface areas of these two sub-peaks with the surface areas of the titanium peak and of the phosphorus peak confirms this hypothesis.

The Ca/P ratio was calculated at the surface and over a thickness of $\sim$ 12 nm. It increases quite quickly within the first nanometres and then becomes more and more constant (Fig. 9). These calcium-poor surfaces observed on ceramics of pure OHAp and β-TCP were already mentioned by different groups [22].

A depth profile over $\sim$ 12 nm, showing the contact region between the bone and the implant, is presented in Fig. 10. The concentration of the different elements is constant. The slow increase of the titanium concentration is due to a sputtering artefact (preferential sputtering of oxygen inducing a reduction of Ti^{4+} in Ti^{3+}).

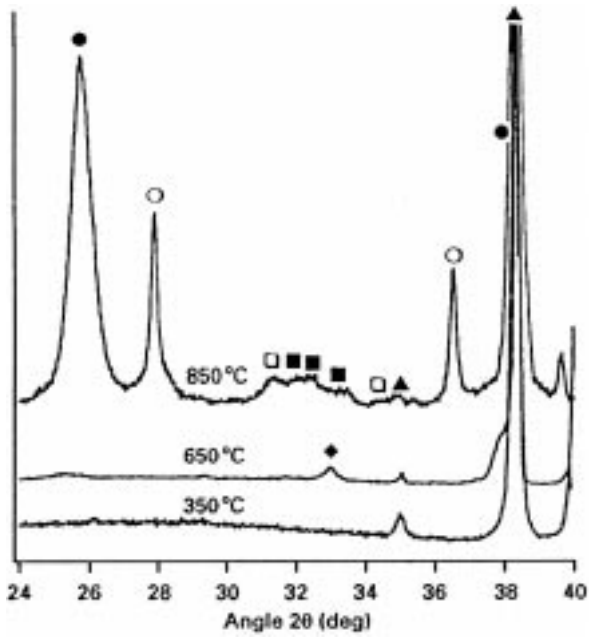

Figure 5 X-ray diffraction pattern of a coating prepared with a solution and crystallized for 10 min at various temperatures: (●) TiO_2 anatase, (○) TiO_2 rutile, (■) OHAp, (□) β-TCP, (◆) $CaTiO_3$, (▲) substrate.

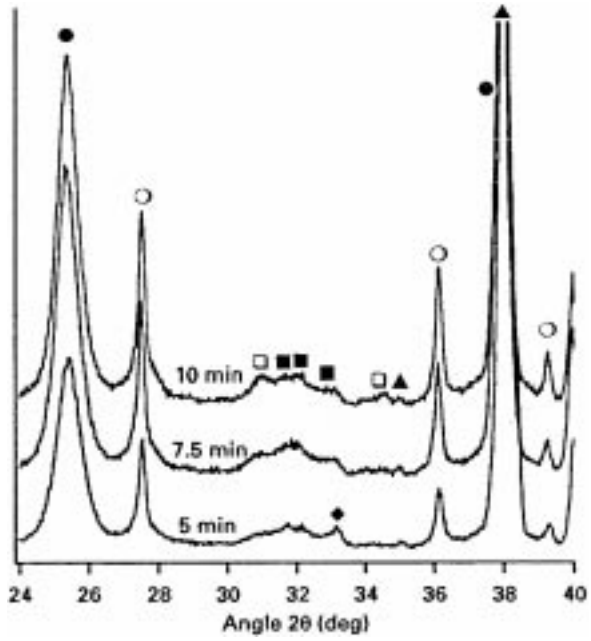

Figure 6 X-ray diffraction pattern of a coating prepared with a solution and crystallized at 850 °C for various times: (●) TiO_2 anatase, (○) TiO_2 rutile, (■) OHAp, (□) β-TCP, (◆) $CaTiO_3$, (▲) substrate.

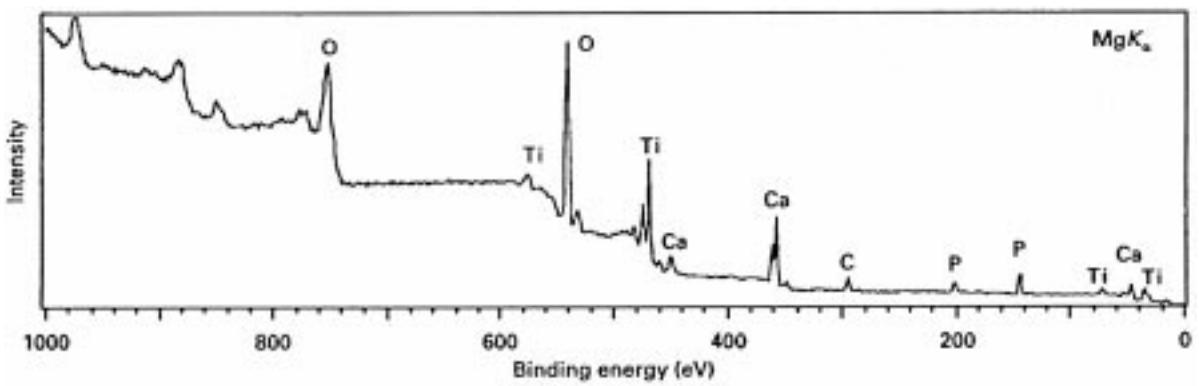

Figure 7 XPS survey spectrum of a coating crystallized for 10 min at 850 °C. The precursor is a sol.

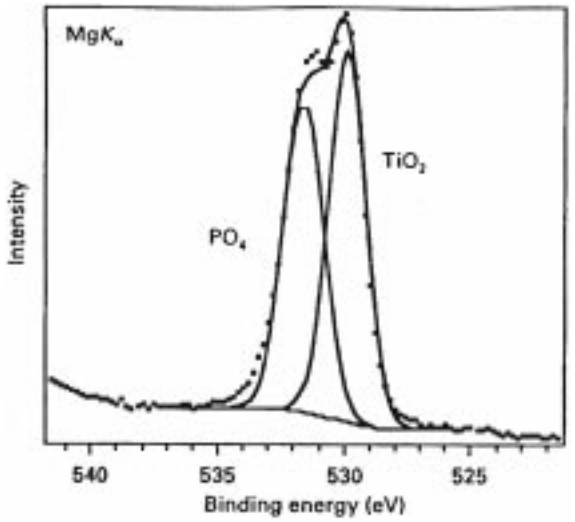

Figure 8 Representative high-resolution XPS spectrum of O (1 s). Peak assignments are TiO_2 at 529.6 eV and PO_4 at 531.1 eV.

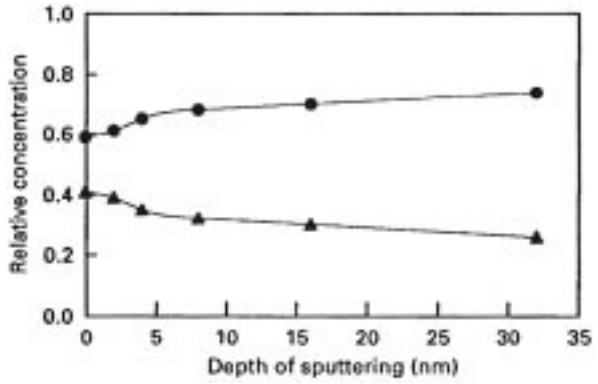

Figure 9 XPS concentration depth profile (element concentration versus depth) of (●) calcium and (▲) phosphorus of a coating prepared with a sol.

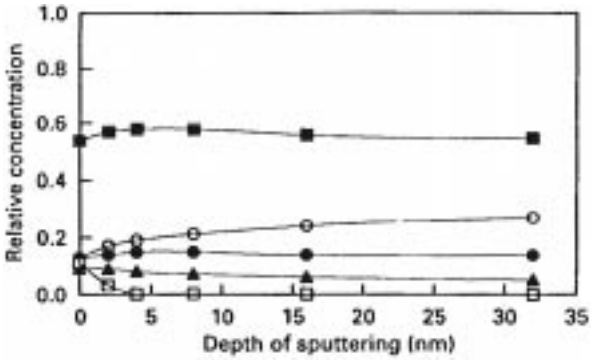

Figure 10 XPS concentration depth profile (element concentration versus depth) of a coating prepared with a sol. (■) Oxygen. (○) titanium. (●) calcium, (▲) phosphorus. (□) carbon.

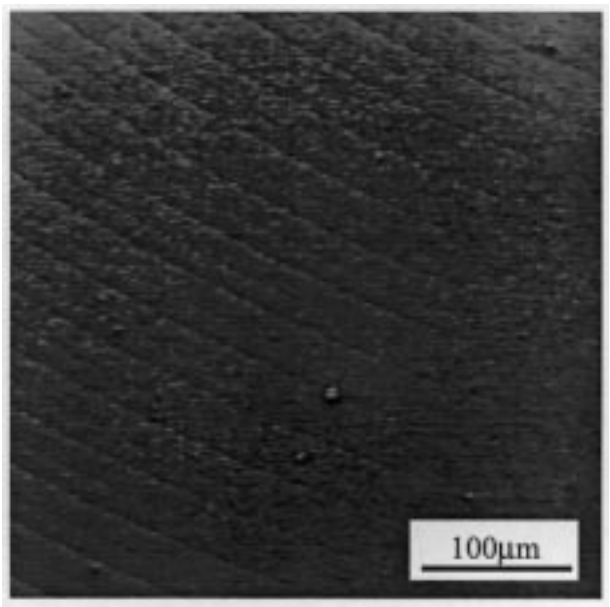

Figure 11 Large-scale scanning electron micrograph of a calcium phosphate titanium dioxide coating produced with a sol precursor and crystallized for 10 min at 850 °C. The microgrooves originate from the mechanical polishing of the sample surface prior to the coating.

3.3. SEM

A systematic study of the surface morphology was performed. Substrates, with various pre-treatments, were coated with films of variable thickness. In such a process, the thickness of the deposited layer is related to the viscosity and also to the concentration of the precursor (e.g. [23]). To vary the thickness of our coatings, and to examine their influence on the morphology, precursors of different concentrations have been used.

Fig. 11 shows a micrograph, at low magnification, of the surface of a coated sample which was previously mechanically polished. The coating is homogeneous and presents a structure analogous to that of the substrate. The grooves are about 20 µm wide and 10 µm deep.

Figs 12 and 13 show the topography of samples with the same type of coating but after different heat treatments. The first one was not crystallized and the second one was crystallized for 10 min at 850 °C. No major changes are observed. Islands, about 10 µm in diameter, are surrounded by deep cracks 2–4 µm wide. A reduction in the roughness is observed on samples coated with thinner films (Fig. 14). The islands become larger and the cracks disappear completely. Some cracks, however, are always present due to the structure of the substrate (right side of the picture). The influence of the surface pre-treatment is shown in Figs 14 and 15. The substrate of Fig. 15 was mechanically polished and blasted with pure crystalline aluminum oxide, while the substrate of Fig. 14 was just mechanically polished.

Films obtained by our process are relatively thin. After a deposition sequence of four layers, their thickness is set between 2 and 10 µm (measured by SEM observation of cross-sections of some samples) depending on the concentration of the starting solution. Owing to the constraints during the calcination period, layers with a thickness greater than 1 µm are fissured. Thus, on a large scale, the roughness is mostly related to the substrate's surface pre-treatment. Structures with minimum sizes of a few micrometres still appear after coating. On a 1–10 µm scale, the main influence is due to the conditions of film fabrication and, in particular, to the solution's viscosity. Upto a certain point, the substrate topography will induce some roughness. Edges and peaks will produce cracks on the films. Reducing the viscosity of the starting solution allows the roughness of the coatings to be reduced. Samples with very different outermost surfaces can also be produced, depending on the requirements.

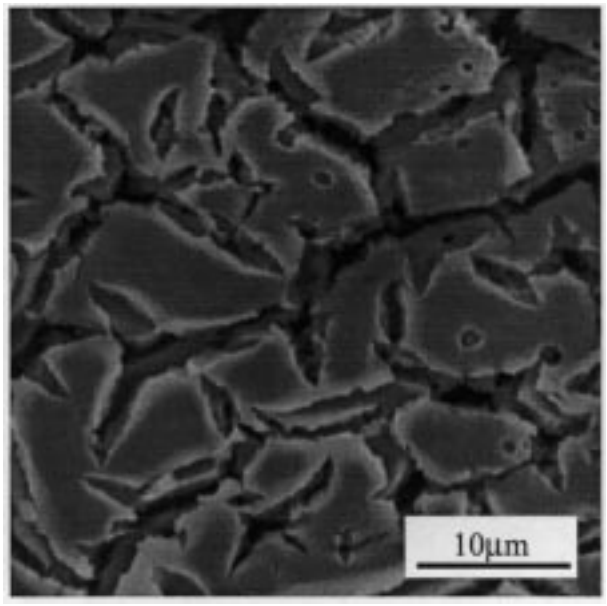

Figure 12 Scanning electron micrograph of a calcium phosphate titanium dioxide coating produced with a concentrated sol precursor (1 M in titanium) before crystallization. The substrate was mechanically polished.

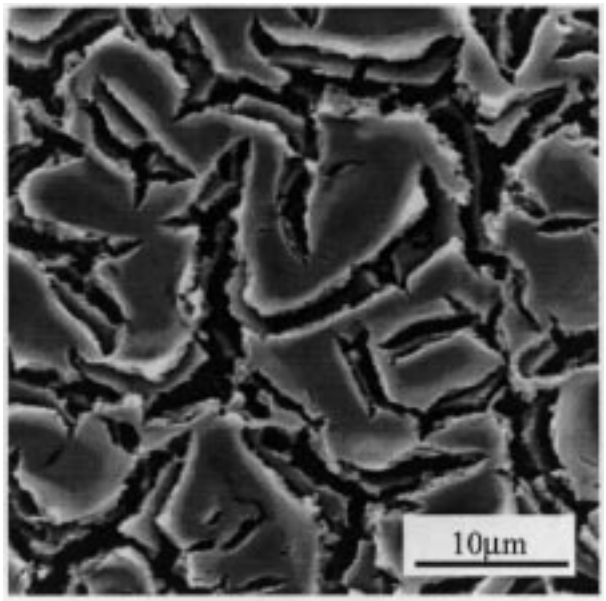

Figure 13 Scanning electron micrograph of a calcium phosphate titanium dioxide coating produced with a concentrated sol precursor (1 M in titanium) after crystallization for 10 min at 850 °C. The substrate was mechanically polished.

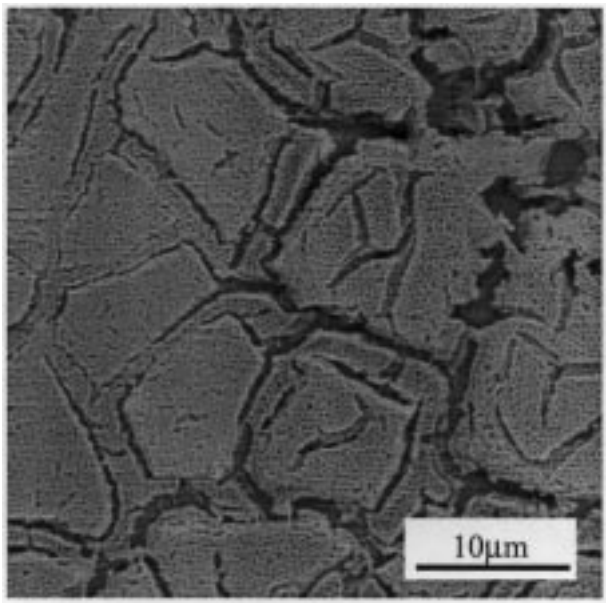

Figure 14 Scanning electron micrograph of a calcium phosphate titanium dioxide coating produced with a diluted sol precursor (0.25 M in titanium) after crystallization for 10 min at 850 °C. The micrograph was taken at the edge of a groove (right side). The substrate was mechanically polished.

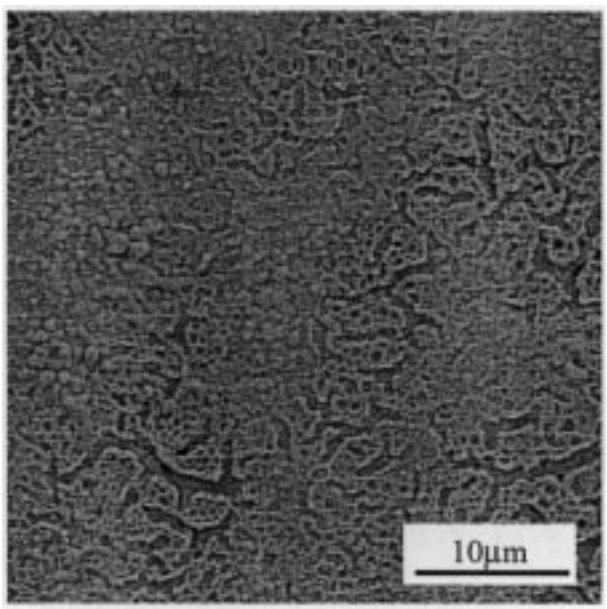

Figure 15 Scanning electron micrograph of a calcium phosphate titanium dioxide coating produced with a diluted sol precursor (0.25 M in titanium) after crystallization for 10 min at 850 °C. The substrate was blasted with aluminum oxide.

4. Conclusion

A sol-gel route was used to produce coatings of titanium dioxide containing calcium phosphate. XRD patterns indicate the presence of crystalline titanium dioxide, of apatite as well as tricalcium phosphate. The importance of the preparation of the precursor is shown. The use of TiO_2 instead of $Ti(OBu)_4$ in the precursor drastically reduces the ability of titanium to react with calcium. Hydrolyzing the titanium also allows a reduction of the firing time and, therefore, of the induced thermal oxidation. This oxidation can affect the mechanical properties of the implant and should be avoided.

The surface chemistry presents a very low contamination. The calcium to phosphorus ratio is lower at the surface and increases within the first 40 nm.

The surface topography of the samples on a micrometre scale is shown to be related to the viscosity of the starting precursor, and to the surface topography of the substrate. A more viscous precursor leads to the formation of rougher layers. Micro-grooves, edges and peaks on the substrate induce an increase in the roughness. However, firing temperature seems to have no clear effect on the roughness.

Acknowledgments

The authors thank F. P. for unfailing support, C. Neururer for SEM images and G. Galetti for XRD spectra. This research was supported by the Dr h.c. Robert Mathys Foundation.

References

1. P.-I. BRÅNFMARK, U. BRYONIA, R. ADELL, B. O. HANSSON, J. LINDSTROM and A. OLSSON, *Scand J. Plast. Reconstr. Surg.* **3** (1969) 81.
2. G. MEACHIM and R. B. PEDLEY, in ''CRC Fundamental Aspects of Biocompatibility'', Vol 1, edited by D. F. Williams (CRC Press, Boca Raton. FL. 1981) p. 107.
3. W. TONG, J. CHEN and X. ZHANG, *Biomaterials* **16** (1995) 829.
4. E. P. PASCHALIS, Q. ZHAO, B. E. TUCKER, S. MUKHOPADHAYAY, J. A. BEARCROFT, N. B. BEALS, M. SPECTOR and G. H. NANCOLLAS, *J. Biomed. Mater. Res.* **29** (1995) 1499.
5. P. CHEANG and K. A. KOHR, *Biomaterials* **17** (1996) 537.
6. P. DUCHFYNF, S. RADIN, M HEUGHEBAFRT and J. C. HEUGHEBAFRT, *Ibid.* **11** (1990) 244.
7. C. M. COTELL, *Appl Surf. Sci.* **69** (1993) 140.
8. M. SHIRKHANZADEH, M. AZADEGAN, V. STACK and S. SCHRFYER, *Mater. Lett.* **18** (1994) 211.
9. A. A. CAMPBELL, G. E. FRYXELL, J. C. LINEHAU and G. I. GRAFF, *J. Biomed. Mater. Res.* **32** (1996) 111.
10. S. W. RUSS, K. A. LUPTAK, C. T. A. SUCHICITAL, T. L. ALFORD and V. B. PIZZICONI, *J. Am. Ceram. Soc.* **79** (1996) 837.
11. T. BRENDEL, A. ENGEL and C. RÜSSEL, *J. Mater. Sci. Mater. Med.* **3** (1992) 175.
12. D. B. HADDOW, P. F. JAMES and R. VAN NOORI, *ibid.* **7** (1996) 255.
13. J. BREME, Y. ZHOU and L. GROH, *Biomaterials* **16** (1995) 239.
14. Q. QIU, P. VINCENT, B. LOWENBERG, M. SAYER and J. E. DAVIES, *Cells Mater.* **3** (1993) 351.
15. L. -D. PIVETEAU, B. GASSER and L. SCHLAPBACH, International Pat. Appl. PCT/CH96/0461 (1996).
16. L. -D. PIVETEAU, I. SCHLAPBACH and B. GASSI R, in ''Thin films and surfaces for bioactivity and biomedical applications'', edited by C. M. Cottel. S. M. Gorbatkin. G. Grove and A. E. Meyer (Materials Research Society. Pittsburgh. PA, 1996) p. 81.
17. C. SCHMUTZ, E. BASSET, P. BARBOUX and J. MAQUET, *J. Mater. Chem.* **3** (1993) 393.
18. ''Powder Diffraction File'', (JCPDS, Swarthmore, PA). T_1O_2 anatase: file 21-1272, T_1O_2 rutile: file 21-1276, CaT_1O_3: file 22-153.
19. ''Handbook of X-ray photoelectron spectroscopy'', edited by G. E. Mullenberg (Perkin-Elmer Corporation, Eden Prairie, MN, 1979).
20. P. M. A. SHERWOOD, in ''Practical Surface Analysis'', Vol. 1. ''Auger and X-ray photoelectron spectroscopy'', edited by D. Briggs and M. P. Seah (Wiley, Chichester, UK 1990) p. 555.
21. G. N. RAIKER, J. C. GREGORY, J. L. ONG, L. C. LUCAS, J. E. LEMONS, D. KAWAHARA and M. NAKAMURA, *J. Vac. Sci. Technol. A* **13** (1995) 2633.
22. A. LEBUGLE and B. SALLEK, in ''Hydroxyapatite and Related Materials'', edited by P. W. Brown and B. Constant (CRC Press, Boca Raton. FL, 1994) p. 319.
23. C. J. BRINKER and G. W. SCHERER, in ''Sol-Gel Science The Physics and Chemistry of Sol-Gel Processing'' (Academic Press, San Diego, CA, 1990).

Received 28 October 1997
and accepted 13 February 1998